

Quasirelativistic energy-consistent 5f-in-core pseudopotentials for divalent and tetravalent actinide elements

Anna Moritz · Xiaoyan Cao · Michael Dolg

Received: 22 March 2007 / Accepted: 27 April 2007 / Published online: 13 June 2007
© Springer-Verlag 2007

Abstract Quasirelativistic energy-consistent 5f-in-core pseudopotentials modeling divalent ($5f^{n+1}$ occupation with $n = 5$ –13 for Pu–No) respectively tetravalent ($5f^{n-1}$ occupation with $n = 1$ –9 for Th–Cf) actinides together with corresponding core-polarization potentials have been generated. Energy-optimized (6s5p4d) and (7s6p5d) valence basis sets as well as 2f1g correlation functions have been derived and contracted to polarized double, triple, and quadruple zeta quality. Corresponding smaller (4s4p) and (5s5p) respectively (4s4p3d) and (5s5p4d) basis sets suitable for calculations on actinide(II) respectively actinide(IV) ions in crystalline solids form subsets of these basis sets designed for calculations on molecules. Results of Hartree–Fock test calculations for actinide di- and tetrafluorides show a satisfactory agreement with calculations using 5f-in-valence pseudopotentials.

Keywords Actinides · Pseudopotentials · Core-polarization potentials · Valence basis sets · Actinide fluorides

1 Introduction

The study of actinide elements, which have many applications such as nuclear power generation, nuclear weapons, and radiotherapy [1], involves several difficulties for both

experimental and theoretical work. While the toxicity, radioactivity, and scarcity of the actinides are the main obstacles for the experimentalists, theoreticians face particular challenges in the significant contributions of relativity as well as electron correlation [2–5].

A commonly used approximation to cope with some of these problems in quantum chemical calculations is the pseudopotential (PP) approach, in which the explicit calculations are restricted to the chemically relevant valence electron system and relativistic effects are only implicitly accounted for by a proper adjustment of free parameters in the valence model Hamiltonian. For actinides two kinds of energy-consistent PPs with different core definitions, i.e., 5f-in-valence [6, 7] and 5f-in-core [8] PPs, are available. The recently published 5f-in-core PPs for trivalent actinide elements avoid all difficulties due to the open 5f shell, and are therefore an efficient computational tool for those actinide compounds, where the 5f shell does not significantly contribute to bonding. Hence, calculations even on large molecules containing several actinides become feasible. Furthermore, the 5f-in-core PPs might be a useful method for preoptimizing structures and getting an overview over low-lying electronic configurations prior to more rigorous studies on individual states including the 5f shell explicitly.

Results of Hartree–Fock (HF) test calculations on actinide(III) monohydrates $An^{3+}-H_2O$ and actinide trifluorides AnF_3 ($An = Ac-Lr$) using the 5f-in-core PPs show reasonable agreement with corresponding 5f-in-valence PP calculations even in the beginning of the actinide series, i.e., the m.a.e. (m.r.e.) in bond lengths and energies amount to maximal 0.03 Å (1%) and 0.09 eV (2%) [8]. A preliminary density functional theory (DFT) study on actinide(III) motexafin complexes ($An-Motex^{2+}$, $An = Ac, Cm, Lr$) also demonstrates that the 5f-in-core approach performs encouragingly well [9]. A similar statement holds for the hydration

Electronic supplementary material The online version of this article (doi:10.1007/s00214-007-0330-6) contains supplementary material, which is available to authorized users.

A. Moritz · X. Cao · M. Dolg (✉)
Institut für Theoretische Chemie, Universität zu Köln,
Greinstr. 4, 50939 Köln, Germany
e-mail: m.dolg@uni-koeln.de

behavior of trivalent actinide ions [10]. Moreover, yet unpublished CCSD(T) results of Cao for the vibrational frequencies of UF₃ obtained using the 5f-in-core PP are within the experimental error bars. Thus, despite the widespread common knowledge that the actinide 5f shell is chemically active and cannot be attributed to the core, we found ample quantitative evidence that such an approximation can be made without too much loss of accuracy for many cases.

Since the 5f orbitals are included in the core, one PP for each oxidation state, or rather, for each corresponding 5f subconfiguration is needed. From a chemical point of view actinide elements are usually trivalent [1], wherefore trivalent PPs corresponding to the presence of 5fⁿ subconfigurations have already been generated for Ac through Lr [8]. Analogous to these recently published 5f-in-core PPs, in this paper we present divalent (5fⁿ⁺¹, n = 5–13 for Pu–No) and tetravalent (5f^{n–1}, n = 1–9 for Th–Cf) 5f-in-core PPs together with various valence basis sets for use in calculations of molecules as well as solids. Furthermore, core-polarization potentials (CPPs) are provided to account for static and dynamic core polarization. Results of HF test calculations using the newly developed divalent and tetravalent PPs with and without CPPs for actinide difluorides AnF₂ (An = Pu–No) and tetrafluorides AnF₄ (An = Th–Cf) are mainly compared to corresponding calculations using 5f-in-valence PPs, since only very little experimental as well as all-electron (AE) data are available.

2 Method

The method of relativistic energy-consistent ab initio pseudopotentials is described in detail elsewhere [6, 11, 12] and will be outlined here only briefly. The valence-only model Hamiltonian for a system with *n* valence electrons and *N* nuclei with charges *Q* is given as

$$H_v = -\frac{1}{2} \sum_i^n \Delta_i + \sum_{i<j}^n \frac{1}{r_{ij}} + \sum_i^n \sum_I^N V_I(r_i) + \sum_{I<J}^N \frac{Q_I Q_J}{R_{IJ}}. \quad (1)$$

Here *i* and *j* are electron indices, *I* and *J* are nuclear indices. *V_I(r_i)* denotes a semilocal effective core potential (ECP) for nucleus *I*

$$V_I(r_i) = -\frac{Q_I}{r_{Ii}} + \sum_l \sum_k A_{lk}^I \exp(-a_{lk}^I r_{Ii}^2) P_l^I. \quad (2)$$

P_l^I is the projection operator onto the Hilbert subspace of nucleus *I* with angular momentum *l*

$$P_l^I = \sum_{m_l} |lm_l\rangle \langle lm_l|. \quad (3)$$

The 5f-in-core PPs corresponding to divalent (5fⁿ⁺¹, n = 5–13 for Pu–No) and tetravalent (5f^{n–1}, n = 1–9 for Th–Cf) actinide atoms were similarly generated as the PPs corresponding to trivalent oxidation states (5fⁿ, n = 0–14 for Ac–Lr) [8]. The 1s–5f shells are included in the PP core, while all orbitals with main quantum number larger than 5 are treated explicitly, i.e., 10 and 12 valence electrons for the divalent and tetravalent situation, respectively. The s-, p-, and d-PPs which are composed of 2 Gaussians each (*k* = 2 in (2), i.e., 12 parameters) were adjusted by a least-squares fit to the total valence energies of 9 and 18 reference states for the divalent and tetravalent case, respectively. The reference data were taken from relativistic AE calculations using the so-called Wood–Boring (WB) scalar-relativistic HF approach. Both AE WB as well as PP calculations were performed with an atomic finite-difference HF scheme [13]. In order to allow for some participation of the 5f orbitals in chemical bonding the f-parts of the PPs are designed to describe partial occupations of the 5f shell, which are larger than the integral occupation number implied by the valency, i.e., 5f^{n+1+q} (n = 5–13 for Pu–No) and 5f^{n–1+q} (n = 1–9 for Th–Cf) with 0 ≤ *q* < 1 for di- and tetravalent actinide atoms, respectively [14]. These f-PPs consist of two types of potentials *V*₁ and *V*₂ which are linear combined as follows [8]

$$V = \left(1 - \frac{m}{14}\right) V_1 + \frac{m}{14} V_2. \quad (4)$$

Here *m* is the integral number of electrons in the 5f orbitals kept in the core, i.e., *m* = *n* + 1 and *m* = *n* – 1 for the di- and tetravalent case, respectively. *V*₁ and *V*₂ model 5f shells, which can and respectively cannot accommodate an additional electron. Thus, *V*₁ is the exact potential for a 5f⁰ occupation in tetravalent Th, whereas *V*₂ is exact for 5f¹⁴ in divalent No. The errors in the total valence energies of finite-difference HF calculations are smaller than 0.1 eV for PPs describing divalent situations. For PPs corresponding to tetravalent oxidation states these errors are smaller than 0.1 and 0.15 eV for s-, p-, d-parts and f-parts, respectively.

To account for both static (polarization of the core at the HF level) and dynamic (core-valence correlation) polarization of the PP core CPPs [15–17] were added to the 5f-in-core PPs. The form of the CPPs used here is

$$V_{\text{CPP}} = -\frac{1}{2} \sum_{\lambda}^N \alpha_D^{\lambda} \vec{f}_{\lambda}^2 \quad (5)$$

with

$$\vec{f}_{\lambda} = -\sum_i \frac{\vec{r}_{i\lambda}}{r_{i\lambda}^3} \omega(r_{i\lambda}) + \sum_{\mu \neq \lambda} Q_{\mu} \frac{\vec{r}_{\mu\lambda}}{r_{\mu\lambda}^3} \omega(r_{\mu\lambda}) \quad (6)$$

and

$$\omega(r) = \left(1 - \exp\left(-\delta r^2\right)\right). \quad (7)$$

Here α_D^λ denotes the dipole polarizability of the PP core λ and \vec{f}_λ is the electric field at this core generated by the valence electrons (at relative positions $\vec{r}_{i\lambda}$) and the other cores or nuclei (with charges Q_μ , at relative positions $\vec{r}_{\mu\lambda}$). Since the validity of the underlying multipole expansion breaks down for small distances from the core λ , the electric field \vec{f}_λ has to be multiplied by a cutoff factor ω . The Dirac–Hartree–Fock (DHF) dipole polarizabilities α_D of Ra^{10+} (1.0407 atomic units [a.u.]) and No^{10+} (6.4819 a.u.) and Th^{12+} (0.7830 a.u.) and Rf^{12+} (2.5179 a.u.) were used to interpolate those of the other An^{10+} and An^{12+} cores, respectively, because the DHF program package [18] can only handle closed-shell systems. Since the dipole polarizabilities of the high-charged PP cores An^{10+} and An^{12+} are strongly dependent on the presence of the valence electrons, the polarizabilities were calculated using the orbitals of the neutral An atoms and the An^{2+} dications with the subconfiguration $6s^2 6p^6 7s^2$. The cutoff parameters δ were fitted to the following ionization potentials (IP) using a coupled-cluster method with single and double excitation operators and a perturbative estimate of triple excitations [CCSD(T)]: $\text{IP}_1 + \text{IP}_2$ of Am and IP_1 , IP_2 of No (divalent PPs); IP_1 , IP_2 of Th and IP_2 , IP_3 of Bk (tetravalent PPs). The reason why these actinide elements were chosen are their unoccupied (Th), half occupied (Am, Bk), respectively fully occupied (No) 5f orbitals. Since in these cases more accurate reference data are available, i.e., 5f-in-valence PP CCSD(T) calculations without spin–orbit coupling using extrapolation to the basis set limit [7]. For the IPs of Th and Bk needed to adjust the tetravalent CPPs standard basis sets (14s13p10d8f6g)/(6s6p5d4f3g) [7] were taken to obtain the 5f-in-valence PP CCSD(T) values. The 5f-in-core calculations were carried out with the MOLPRO program package [19] using (10s10p10d8f6g) even-tempered basis sets, which were CCSD(T) energy-optimized for the $6d^1 7s^1$ and $6d^2 7s^2$ valence subconfiguration of the neutral atoms for the PPs describing divalent and tetravalent oxidation states, respectively. The cutoff parameters δ of the other actinide elements were interpolated using the values of Am (0.6980)/No (0.2404) and Th (0.9293)/Bk (0.4867), respectively.

The Gaussian type orbital (GTO) valence basis sets for the divalent and tetravalent 5f-in-core PPs were constructed analogous to those for the trivalent PPs [8]. But here only two different sets of primitive Gaussian functions (6s5p4d) and (7s6p5d) were derived, since the (8s7p6d) basis sets for the trivalent PPs yield results, which are almost of the same quality as those of the (7s6p5d) basis sets. First, basis sets for use in crystal calculations were created, i.e., in the divalent case (4s4p) and (5s5p) basis sets were HF energy-optimized [20] for the $6s^2 6p^6$ valence subconfiguration

of doubly-charged actinide cations, and in the tetravalent case (4s4p3d) and (5s5p4d) basis sets were HF energy-optimized [20] for the $6s^2 6p^6 6d^1$ valence subconfiguration of triply-charged actinide cations. All exponents, which became smaller than 0.15, were fixed to this value and the remaining exponents were reoptimized. Furthermore, all optimizations were carried out with the requirement that the ratio of exponents in the same angular symmetry must be at least 1.5. The basis set errors in the valence energies are at most 0.11 and 0.03 eV for (4s4p) and (5s5p), respectively, as well as 0.14 and 0.07 eV for (4s4p3d) and (5s5p4d), respectively.

Secondly, the valence basis sets were augmented by adding a set of 2s1p4d and 2s1p5d low-exponent Gaussians to (4s4p) and (5s5p), respectively, as well as a set of 2s1p1d to (4s4p3d) and (5s5p4d) yielding final (6s5p4d) and (7s6p5d) primitive sets for use in molecular calculations. The added exponents were HF energy-optimized [20] for the $7s^2$ (s-basis), $7s^1 7p^1$ (p-basis), and $6d^1 7s^1$ (d-basis) valence subconfiguration of the divalent PPs as well as for the $6d^2 7s^2$ valence subconfiguration of the tetravalent PPs. The differences in the valence energies are at most 0.15 and 0.04 eV for (6s5p4d) and (7s6p5d) of the divalent PPs, respectively. In case of tetravalent PPs the differences are at most 0.13 and 0.08 eV for these two basis sets.

Thirdly, the basis sets were contracted using different segmented contraction schemes to yield basis sets of approximately valence double, triple, and quadruple zeta quality (VDZ, VTZ, and VQZ) for the s and p symmetries. In case of d symmetry at least a triple zeta contraction was necessary and additional sets with less tight d contraction are also offered (VDZ: [4s3p3d], VTZ: [5s4p3d], [5s4p4d], and VQZ: [6s5p4d]). The errors in total valence energies of the $6d^1 7s^1$ (divalent) and $6d^2 7s^2$ (tetravalent) valence substates of all contracted basis sets are below 0.2 eV. In the case of the divalent PPs all contractions of the (7s6p5d) and for the tetravalent case the VQZ contraction of (7s6p5d) yield errors smaller than 0.1 eV.

Fourthly, sets of 2f1g correlation/polarization functions were energy-optimized in configuration interaction (CI) calculations [19] for the $7s^2$ and $6d^2 7s^2$ valence subconfiguration for divalent and tetravalent PPs, respectively. The exponents of Pu and Fm–No (divalent PPs) as well as of Th, Pa, and Bk (tetravalent PPs) were calculated explicitly, while those of Am–Es (divalent PPs) as well as of U–Cm and Cf (tetravalent PPs) were interpolated. The parameters of PPs, CPPs, and basis sets are compiled in the electronic supplementary material of this publication. They are also available from the authors and will be incorporated, e.g., into the MOLPRO [19] basis set library.¹

The test calculations for AnF_2 (An = Pu–No) and AnF_4 (An = Th–Cf) were carried out with MOLPRO [19] using

¹ <http://www.theochem.uni-stuttgart.de/pseudopotentials>.

divalent respectively tetravalent 5f-in-core LPPs (large-core PP with 10 respectively 12 valence electrons and 84–92 (Pu–No) respectively 78–86 (Th–Cf) core electrons) with and without CPPs as well as 5f-in-valence SPPs [6] (small-core PP with 60 core electrons and 34–42 (Pu–No) respectively 30–38 (Th–Cf) valence electrons). For F Dunning's aug-cc-pVQZ (augmented correlation-consistent polarized VQZ) basis set [21,22] was applied and for An (7s6p5d2f1g)/[6s5p4d2f1g] and (14s13p10d8f6g)/[6s6p5d4f3g] [7] valence basis sets were used for LPP and SPP calculations, respectively. The AnF₂ geometries were optimized within the C_{2v} symmetry and the AnF₄ structures within the T_d point group using HF and state-averaged multiconfiguration self-consistent field (MCSCF) for LPP and SPP, respectively. The state-averaging was necessary to avoid symmetry-breaking at the orbital level, since the program MOLPRO [19] is limited to the D_{2h} point group and subgroups. In the case of ThF₄ and UF₄, for which experimental bond lengths are available [23,24], LPP CCSD(T) calculations with and without CPPs were carried out, too.

3 Results and discussion

The results for some properties (namely the bond length R_e , the bond angle \angle , and the bond energy E_{bond}) of AnF₂ (An = Pu–No) as well as of AnF₄ (An = Th–Cf) will be presented here to demonstrate the transferability of the 5f-in-core PPs, the CPPs, and the corresponding basis sets to a molecular environment.

The actinide–fluorine bond energy was calculated by $E_{\text{bond}} = [E(\text{An}) + n \times E(\text{F}) - E(\text{AnF}_n)]/n$ (with $n = 2, 4$ for AnF₂, AnF₄), where the actinide atom was assumed to be in the lowest valence substate, i.e., 5f^{*n*+1}7s² and 5f^{*n*-1}6d²7s² for AnF₂ and AnF₄, respectively. At this point one might ask how to calculate a binding energy with respect to the experimentally observed ground states of the actinides, e.g., at the correlated level. We suggest to follow the strategy proposed for the lanthanide PPs almost two decades ago [25]. First, one should calculate the binding energy with respect to the actinide atom in its lowest valence substate corresponding to the 5f^{*n*+1} and 5f^{*n*-1} subconfiguration (i.e., 5f^{*n*+1}7s² and 5f^{*n*-1}6d²7s²) for di- and tetravalent LPPs, respectively. Then the energy difference to the experimentally observed ground state, possibly belonging to a different configuration, can be determined, e.g., at the AE WB [13] or DHF level [26], and corrected by electron correlation contributions to the energy difference (between the lowest levels) taken from experiment.² If desired, correlation contributions can of course also be obtained by 5f-in-valence PP or AE calculations thus eliminating any empirical corrections. Tables

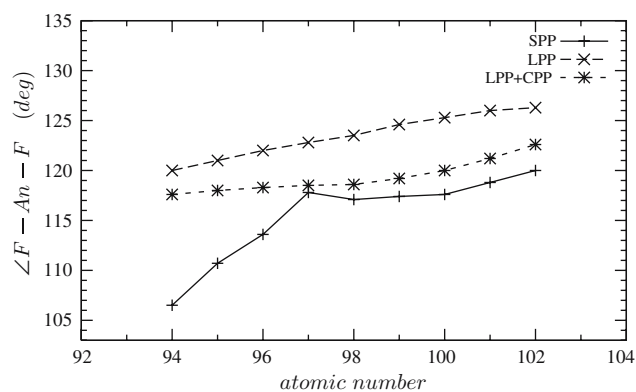


Fig. 1 Actinide–fluorine bond angles $\angle\text{F–An–F}$ (in degrees) for AnF₂ (An = Pu–No) from LPP HF calculations with and without using CPPs as well as from SPP state-averaged MCSCF calculations. Basis sets: LPP (7s6p5d2f1g)/[6s5p4d2f1g]; SPP (14s13p10d8f6g)/[6s6p5d4f3g]; F aug-cc-pVQZ

summarizing some possible corrections are included in the electronic supplementary material.

3.1 Actinide difluorides

The HF calculations for AnF₂ (An = Pu–No) using LPPs with and without CPPs will be compared to corresponding SPP calculations. The comparison is reasonable for the late actinides, but due to mixing of 5f with 7s as well as 6d orbitals in the case of the SPP calculations critical for the lighter actinides. This can best be seen from the calculated bond angles, which show much larger discrepancies for Pu–Cm than for Bk–No (cf. Fig. 1). Hence, all results will be compared separately for the elements Pu–Cm and Bk–No, respectively. The results of a Mulliken population analysis and those for bond lengths and angles as well as binding energies of the LPP, LPP + CPP, and SPP calculations are listed in Tables 1 and 2, respectively.

3.1.1 Mulliken orbital populations

Table 1 shows the Mulliken orbital populations obtained by LPP HF and SPP state-averaged MCSCF calculations, respectively. As one can see the bonding of AnF₂ is of polar covalent nature, i.e., the two binding electron pairs are dragged more close to the fluorines ends of the bonds. For the LPP calculations this results in charge separations of up to 0.90 electrons per bond and a total atomic charge of up to 1.80 units on the actinide. Whereas the s, p, and f occupation numbers on the actinides are nearly integral, those of the d shells are not and point to some covalent contributions. The SPP f orbital occupations show that there is almost no 5f orbital participation in the bonding of AnF₂ with An = Cm–No, since the SPP 5f populations differ at most by 0.02 electrons from the integral LPP 5f occupations. However, for PuF₂

² <http://www.lac.u-psud.fr/Database/Contents.html>.

Table 1 Mulliken 6s/7s, 6p/7p, 6d, and 5f orbital populations and atomic charges (Q) on An in AnF₂ (An = Pu–No) from LPP HF and SPP state-averaged MCSCF calculations

| An | s | | p | | d | | f | | Q | |
|----|------|------|------|------|------|------|------------------|-------|------|------|
| | LPP | SPP | LPP | SPP | LPP | SPP | LPP ^a | SPP | LPP | SPP |
| Pu | 2.00 | 2.16 | 6.00 | 6.00 | 0.21 | 0.37 | 0.02 | 5.90 | 1.78 | 1.57 |
| Am | 2.00 | 2.12 | 6.00 | 6.00 | 0.21 | 0.32 | 0.01 | 6.97 | 1.78 | 1.58 |
| Cm | 2.00 | 2.12 | 5.99 | 6.00 | 0.20 | 0.30 | 0.01 | 8.00 | 1.79 | 1.59 |
| Bk | 2.00 | 2.12 | 5.99 | 6.01 | 0.20 | 0.28 | 0.01 | 9.01 | 1.79 | 1.59 |
| Cf | 2.00 | 2.13 | 5.99 | 6.01 | 0.19 | 0.28 | 0.01 | 10.01 | 1.80 | 1.57 |
| Es | 2.01 | 2.14 | 5.99 | 6.02 | 0.19 | 0.27 | 0.01 | 11.01 | 1.80 | 1.56 |
| Fm | 2.01 | 2.14 | 5.99 | 6.02 | 0.19 | 0.27 | 0.01 | 12.02 | 1.80 | 1.54 |
| Md | 2.01 | 2.15 | 5.99 | 6.02 | 0.18 | 0.26 | 0.01 | 13.01 | 1.80 | 1.56 |
| No | 2.02 | 2.15 | 5.99 | 6.02 | 0.18 | 0.25 | 0.01 | 14.01 | 1.80 | 1.57 |

A 6s²6p⁶7s² ground state valence subconfiguration is considered for An. Basis sets: LPP (7s6p5d2f1g)/[6s5p4d2f1g]; SPP (14s13p10d8f6g)/[6s6p5d4f3g]; F aug-cc-pVQZ

^a 6–14 electrons in the 5f shell are attributed to the LPP core for Pu–No, respectively

Table 2 Actinide–fluorine bond lengths R_e (in Å) and angles $\angle F-An-F$ (in degrees) as well as bond energies E_{bond} (in eV) for AnF₂ (An = Pu–No) from LPP HF calculations with and without using CPPs as well as from SPP state-averaged MCSCF calculations

| An | R_e | | | $\angle F-An-F$ | | | E_{bond} | | |
|----|--------------|------------------|--------------|-----------------|------------------|--------------|-------------------|------------------|--------------|
| | LPP | CPP ^a | SPP | LPP | CPP ^a | SPP | LPP | CPP ^a | SPP |
| Pu | 2.212 | 2.179 | 2.152 | 120.0 | 117.6 | 106.5 | 3.764 | 3.644 | 4.057 |
| Am | 2.200 | 2.164 | 2.163 | 121.0 | 118.0 | 110.7 | 3.715 | 3.605 | 3.907 |
| | <i>2.182</i> | <i>2.157</i> | <i>2.089</i> | <i>116.7</i> | <i>114.6</i> | <i>104.3</i> | <i>5.188</i> | <i>5.209</i> | <i>5.517</i> |
| Cm | 2.189 | 2.150 | 2.161 | 122.0 | 118.3 | 113.6 | 3.667 | 3.571 | 3.836 |
| Bk | 2.178 | 2.137 | 2.155 | 122.8 | 118.5 | 117.8 | 3.617 | 3.540 | 3.764 |
| Cf | 2.168 | 2.127 | 2.144 | 123.5 | 118.6 | 117.1 | 3.564 | 3.507 | 3.705 |
| Es | 2.156 | 2.116 | 2.134 | 124.6 | 119.2 | 117.4 | 3.517 | 3.476 | 3.611 |
| Fm | 2.146 | 2.110 | 2.122 | 125.3 | 120.0 | 117.6 | 3.464 | 3.434 | 3.540 |
| Md | 2.136 | 2.106 | 2.120 | 126.0 | 121.2 | 118.8 | 3.409 | 3.380 | 3.468 |
| No | 2.128 | 2.105 | 2.118 | 126.3 | 122.6 | 120.0 | 3.347 | 3.312 | 3.375 |
| | <i>2.114</i> | <i>2.100</i> | <i>2.057</i> | <i>121.2</i> | <i>118.9</i> | <i>112.5</i> | <i>4.790</i> | <i>4.833</i> | <i>5.043</i> |

For AmF₂ and NoF₂ LPP CCSD(T) results with and without using CPPs as well as SPP CCSD(T) results are given in italics. Basis sets: LPP (7s6p5d2f1g)/[6s5p4d2f1g]; SPP (14s13p10d8f6g)/[6s6p5d4f3g]; F aug-cc-pVQZ. In the CCSD(T) calculations the F 1s orbitals were frozen

^a LPP calculations using CPPs

and AmF₂ the SPP calculations do not yield 5f occupations corresponding to a divalent actinide, i.e., the 5f populations are 0.10/0.03 electrons below the integral number of 5f electrons for Pu/Am. This is due to the stronger mixing between 5f and 7s as well as 6d orbitals for these lighter actinides, where the 5f orbitals are still relatively diffuse. The mixing of 5f with 6d orbitals, which can also be seen as a configurational mixing of 5f^{*n*+1} and 5f^{*n*}6d¹, decreases from Pu to No, since the 6d orbitals are destabilized due to the indirect relativistic effect, and are thus less occupied (6d AE WB orbital energies for 5f^{*n*+1}6s²6p⁶6d¹7s¹: −3.123/−2.311 eV for Pu/No; 6d occupation for SPP: 0.37/0.25 for Pu/No). Therefore the

LPP results are expected to become better with increasing nuclear charge and to be less accurate for the lighter actinides Pu–Cm, where the 5f occupation falls below the assumed integral value corresponding to a divalent actinide.

3.1.2 Actinide difluoride structure

For all AnF₂ (An = Pu–No) non-linear structures were obtained by both LPP and SPP calculations. In the case of the LPP calculations for increasing nuclear charge of the actinide the bond lengths decrease almost linearly (correlation coefficient 0.999) by 0.08 Å and the bond angles increase by

6°. These smooth variations are due to the actinide contraction and the increasing repulsion between the fluorine atoms, respectively. Similar trends are also observed for the SPP results, i.e., bond lengths decrease and bond angles increase by 0.03 Å and 14°, respectively, however here two irregularities appear. On the one hand the bond length increases instead of decreases from Pu to Am by 0.01 Å, and on the other hand the bond angles between Pu and Bk increase on average by 4°, while those between Bk and No grow only by about 0.4°. The reason for both is a mixing of 5f with 7s as well as 6d orbitals, which becomes more significant with decreasing nuclear charge, and as already mentioned above limits the applicability of the 5f-in-core approach.

A comparison of actinide–fluorine bond lengths calculated using LPPs and SPPs demonstrates that the newly developed LPPs yield quite accurate results for all actinides considered. The bond lengths are on average by 0.042 (0.020) Å and 1.9 (0.9)% too long for Pu–Cm (Bk–No). The actinide–fluorine bond angles $\angle F\text{--}An\text{--}F$, which are also overestimated by using LPPs, show clearly larger deviations. The mean absolute error (m.a.e.) and the mean relative error (m.r.e.) for Pu–Cm (Bk–No) amount to 10.7° (6.6°) and 10% (6%), respectively. The largest deviations for both bond length and angle occur for Pu (0.059 Å; 13.5°) and Am (0.037 Å; 10.3°), since here the actual 5f occupation is smaller than the integral value modeled by the LPP core (cf. Table 1).

The use of LPPs in connection with CPPs gives about 0.036 Å and 4.2° smaller bond lengths and angles, respectively. Since pure LPP calculations overestimate the An–F bond lengths by ca. 0.027 Å, they are underestimated by ca. 0.015 Å using LPPs in combination with CPPs (m.a.e. for Pu–No). Considering the deviations in bond lengths for Pu–Cm and Bk–No separately, one finds a clear improvement by using CPPs in the case of Pu–Cm, i.e., the mean deviation related to the SPP data decreases by 0.029 Å (m.a.e.: LPP/LPP+CPP 0.042/0.013 Å). For Bk–No, however, this deviation remains almost constant, i.e., the improvement in the m.a.e. amounts to 0.005 Å (m.a.e.: LPP/LPP+CPP 0.020/0.015 Å). In the case of the bond angles the decrease by using CPPs reduces the errors of the LPP calculations for all actinides considered, i.e., the m.a.e. for Pu–No drops from 8.0 to 3.9°.

3.1.3 Actinide–fluorine bond energy

The actinide–fluorine bond energy of AnF_2 decreases by 0.42 and 0.68 eV with increasing nuclear charge for LPP and SPP calculations, respectively. This is related to the decreasing actinide–fluorine bond length, which is accompanied by an increasing fluorine–fluorine repulsion.

The differences in the actinide–fluorine bond energies between LPP and SPP calculations for the lighter actinides are

obviously larger than those for the heavier actinides, i.e., the m.a.e. and m.r.e. for Pu–Cm (Bk–No) are 0.218 (0.091) eV and 5.5 (2.5)%, respectively. This is most likely due to a mixing of valence 5f with mainly valence 7s and 6d orbitals in the SPP state-averaged MCSCF calculations. Analogous to the bond lengths and angles the largest errors occur for Pu (0.293 eV, 7.2%) and Am (0.192 eV, 4.9%), where the SPP 5f occupations are smaller than the assumed integral LPP 5f occupations (cf. Table 1).

The application of CPPs causes a mean decrease in bond energy of 0.066 eV compared to pure LPP calculations. Since the bond energy is already underestimated by using LPPs without CPPs, the deviations from SPP calculations become larger by using CPPs. The m.a.e. (m.r.e.) amounts to 0.326 eV (8.3%) and 0.136 eV (3.7%) for Pu–Cm and Bk–No, respectively, compared to those for pure LPP calculations of 0.218 eV (5.5%)/0.091 eV (2.5%) for Pu–Cm/Bk–No. The strong energy decrease due to CPPs can be explained, if one thinks of an ionic bond energy

$$E_{bond} = -IP_1(An) - IP_2(An) + 2 \times EA(F) + \text{ionic interaction.} \quad (8)$$

Here, $IP_i(An)$ with $i = 1, 2$ are the first respectively second ionization potential of the actinide and $EA(F)$ is the electron affinity of fluorine. The use of CPPs increases the IPs, because the actinide atom or ion is stabilized via the included correlation, and thus the bond energy is reduced. The first and second IP of the actinides Pu–No from LPP state-averaged MCSCF respectively LPP CCSD(T) calculations with and without using CPPs in comparison to SPP state-averaged MCSCF [7] respectively experimental³ and SPP multireference averaged coupled-pair functional (ACPF) [7] data are listed in Table 3. The IPs of Cm are omitted, because its ionizations do not take place between divalent oxidation states, i.e., the Cm atom respectively Cm^+ ion does not have a $5f^{n+1}$, but a $5f^n$ occupation. As one can see IP_1 and IP_2 are increased by about 0.32 and 0.50 eV, respectively, if LPP+CPP instead of LPP state-averaged MCSCF calculations are performed. The pure LPP IPs deviate only on average by 0.09/0.12 eV from the SPP values for IP_1/IP_2 , however, using CPPs the IPs are overestimated by about 0.39/0.38 eV. The reason for the worse IP results using CPPs, which explain the larger deviations in An–F bond energies, might be the inclusion of dynamic correlation. Since the CPPs are adjusted to CCSD(T) reference data, they account for both static (polarization at the HF level) and dynamic (core-valence correlation) polarization of the PP core, even if they are applied in HF respectively state-averaged MCSCF calculations. The SPP state-averaged MCSCF calculations, however, do not

³ <http://www.physics.nist.gov/PhysRefData/IonEnergy/tblNew.html>.

Table 3 First and second ionization potential (in eV) of the divalent actinides Pu–No (except for Cm) from LPP state-averaged MCSCF respectively LPP CCSD(T) calculations with and without using CPPsin comparison to SPP state-averaged MCSCF [7] respectively experimental (<http://www.physics.nist.gov/PhysRefData/IonEnergy/tblNew.html>) and SPP ACPF data [7]

| An | SCF level | | | | | | Correlated level | | | | | |
|----|------------------------------|------------------|------|------------------------------|------------------|-------|------------------------------|------------------|------|------------------------------|------------------|------------------|
| | IP ₁ ^a | | | IP ₂ ^a | | | IP ₁ ^a | | | IP ₂ ^a | | |
| | LPP | CPP ^b | SPP | LPP | CPP ^b | SPP | LPP | CPP ^b | exp. | LPP | CPP ^b | SPP ^c |
| Pu | 4.91 | 5.22 | 4.73 | 10.65 | 11.18 | 10.84 | 5.77 | 5.89 | 6.03 | 11.27 | 11.53 | 11.54 |
| Am | 4.97 | 5.30 | 4.77 | 10.80 | 11.36 | 11.02 | 5.84 | 5.96 | 5.97 | 11.42 | 11.69 | 11.69 |
| Bk | 5.11 | 5.46 | 4.99 | 11.10 | 11.66 | 11.25 | 5.98 | 6.10 | 6.20 | 11.72 | 11.97 | 11.96 |
| Cf | 5.18 | 5.53 | 5.09 | 11.24 | 11.79 | 11.34 | 6.04 | 6.17 | 6.28 | 11.86 | 12.10 | 12.02 |
| Es | 5.25 | 5.59 | 5.21 | 11.40 | 11.92 | 11.50 | 6.11 | 6.23 | 6.42 | 12.01 | 12.25 | 12.16 |
| Fm | 5.32 | 5.64 | 5.34 | 11.54 | 12.03 | 11.66 | 6.18 | 6.30 | 6.50 | 12.16 | 12.39 | 12.33 |
| Md | 5.39 | 5.69 | 5.41 | 11.69 | 12.12 | 11.75 | 6.25 | 6.37 | 6.58 | 12.31 | 12.52 | 12.42 |
| No | 5.46 | 5.71 | 5.51 | 11.84 | 12.18 | 11.88 | 6.33 | 6.43 | 6.65 | 12.45 | 12.64 | 12.52 |

Basis sets: LPP (7s6p5d2f1g)/[6s5p4d2f1g]; SPP (14s13p10d8f6g)/[6s6p5d4f3g]

^a Initial and final states: IP₁: $5f^{n+1}7s^2 \rightarrow 5f^{n+1}7s^1$; IP₂: $5f^{n+1}7s^1 \rightarrow 5f^{n+1}7s^0$ ^b LPP calculations using CPPs^c The 5s, 5p, and 5d shells were frozen in the SPP ACPF calculations

include any correlation effects. Thus, the IPs calculated by using CPPs become too large and the corresponding bond energies are too small. However, at the correlated level the experimental respectively SPP ACPF IPs are always underestimated by the LPP CCSD(T) results (m.a.e.: 0.27/0.18 eV for IP₁/IP₂). Therefore the application of CPPs yields improved results, i.e., the m.a.e. is reduced to 0.15/0.06 eV for IP₁/IP₂.

A slight improvement due to CPPs is also found in CCSD(T) calculations for AmF₂ and NoF₂, in which the F 1s orbitals were frozen (cf. Table 2). Here, the deviations from the SPP bond energies amount to 0.329/0.308 eV and 0.253/0.210 eV for LPP/LPP+CPP calculations of AmF₂ and NoF₂, respectively. Furthermore, the LPP+CPP bond lengths and bond angles are also in better agreement with the SPP data than the pure LPP results (differences between SPP and LPP/LPP+CPP: AmF₂: $\Delta R_e = 0.093/0.068$ Å; $\Delta \angle = 12.4/10.3^\circ$; NoF₂: $\Delta R_e = 0.057/0.043$ Å; $\Delta \angle = 8.7/6.4^\circ$). The deviations in bond energies amount to ca. 10% for PuF₂ and decay to ca. 2% when going to NoF₂. Aside from the limited validity of the 5f-in-core approach for PuF₂ and AmF₂, the deviations can be explained by the larger basis set superposition error (BSSE) of the SPP compared to the LPP/LPP+CPP calculations at the CCSD(T) level. Using the counterpoise correction the SPP bond energies are reduced from 5.517/5.043 to 5.319/4.777 eV corresponding to a BSSE of 0.198/0.266 eV for AmF₂/NoF₂. These are reasonable amounts for the BSSE, since the (14s13p10d8f6g)/[6s6p5d4f3g] basis sets [7] recover only about 80% of the atomic CCSD(T) correlation energy. In the case of the LPP CCSD(T) calculations the counterpoise correction yields by 0.041/0.039 eV smaller

bond energies, i.e., the energies are reduced from 5.188/4.790 to 5.147/4.751 eV for AmF₂/NoF₂. Thus, the BSSE using LPPs are clearly smaller than using SPPs, which constitutes an enormous advantage compared to the SPP calculations. Taking the BSSE into account the deviations in bond energies related to the SPP data are reduced to 0.172/0.151 and 0.026/0.017 eV for LPP/LPP+CPP calculations of AmF₂ and NoF₂, respectively. Hence, at the correlated level the LPP bond energies with and without using CPPs are in good agreement with the reference data, and the use of CPPs shows an improvement of the results.

3.2 Actinide tetrafluorides

The HF and CCSD(T) calculations for AnF₄ (An = Th–Cf) using LPPs with and without CPPs will be compared to SPP results and experimental data [23, 24]. The Mulliken orbital population analysis will not be discussed in detail, because it leads to similar conclusions as for AnF₂. However, the 5f orbital populations will be given together with the other results as well as the available experimental data in Table 4.

3.2.1 Actinide–fluorine bond length

The actinide–fluorine bond lengths calculated by using LPPs decrease almost linearly (correlation coefficient 0.995) with increasing nuclear charge, whereby the decrease from ThF₄ to CfF₄ amounts to 0.09 and 0.11 Å for LPP HF and SPP state-averaged MCSCF calculations, respectively. Since for AnF₄ as well as for AnF₂ nine actinide elements, i.e., Th–Cf respectively Pu–No, are considered, one can compare the

Table 4 Actinide–fluorine bond lengths R_e (in Å), bond energies E_{bond} (in eV), and f orbital occupations for AnF_4 (An=Th–Cf) from LPP HF calculations with and without using CPPs in comparison to experimental respectively estimated data [24,23] as well as SPP state-averaged MCSCF calculations

| An | R_e | | | | E_{bond} | | | f occupation | |
|----|--------------|------------------|-------|-------------------|-------------------|------------------|-------|------------------|------|
| | LPP | CPP ^a | SPP | exp. ^b | LPP | CPP ^a | SPP | LPP ^c | SPP |
| Th | 2.107 | 2.101 | 2.115 | 2.124 | 5.617 | 5.630 | 5.571 | 0.27 | 0.28 |
| | <i>2.101</i> | <i>2.097</i> | | | <i>7.117</i> | <i>7.152</i> | | | |
| Pa | 2.104 | 2.098 | 2.092 | | 5.422 | 5.426 | 5.451 | 0.20 | 1.23 |
| U | 2.094 | 2.088 | 2.072 | 2.059 | 5.311 | 5.310 | 5.379 | 0.16 | 2.22 |
| | <i>2.091</i> | <i>2.088</i> | | | <i>6.813</i> | <i>6.839</i> | | | |
| Np | 2.082 | 2.075 | 2.059 | 2.04 | 5.240 | 5.237 | 5.254 | 0.15 | 3.22 |
| Pu | 2.070 | 2.063 | 2.047 | 2.03 | 5.188 | 5.183 | 5.146 | 0.13 | 4.22 |
| Am | 2.057 | 2.050 | 2.035 | 2.02 | 5.152 | 5.147 | 5.057 | 0.12 | 5.22 |
| Cm | 2.044 | 2.037 | 2.026 | | 5.131 | 5.124 | 4.980 | 0.12 | 6.21 |
| Bk | 2.031 | 2.024 | 2.017 | | 5.118 | 5.112 | 4.880 | 0.11 | 7.19 |
| Cf | 2.020 | 2.013 | 2.001 | | 5.106 | 5.099 | 5.037 | 0.11 | 8.19 |

For ThF_4 and UF_4 LPP CCSD(T) results with and without using CPPs are given in italics

Basis sets: LPP (7s6p5d2f1g)/[6s5p4d2f1g]; SPP (14s13p10d8f6g)/[6s6p5d4f3g]; F aug-cc-pVQZ

^a LPP calculations using CPPs

^b For Np, Pu, Am the values are estimated

^c 0–8 electrons in the 5f shell are attributed to the LPP core for Th–Cf, respectively

actinide contraction for these compounds. In the case of AnF_4 the contraction is somewhat larger than that for AnF_2 (AnF_2 contraction: 0.08/0.03 Å for LPP/SPP). The reason for this is that the An–F bond in AnF_2 is more ‘rigid’ [27] as can be seen from a comparison of the force constants, e.g., for LPP HF calculations the force constants are 0.06427 and 0.05843 a.u. for PuF_2 and PuF_4 , respectively.

The LPP HF results are in good agreement with the SPP reference data, i.e., the actinide–fluorine distances determined using LPPs are at most 0.023 Å (1.1%) too long. The m.a.e. and the m.r.e. amount to 0.018 Å and 0.9%, respectively. For CmF_4 the LPP HF result differs by 0.022 Å (1.1%) from the AE DHF bond length 2.022 Å [28] determined by using (28s28p19d13f2g) and (13s9p3d) basis sets for Cm and F, respectively. Compared to the experimental (Th, U) respectively estimated (Np–Am) values the LPP HF calculations yield also satisfactory results, i.e., the m.a.e. (m.r.e.) amount to 0.034 Å (1.7%). The obtained An–F bond lengths (An = Th, U–Am) are also in good agreement with those determined by an interioric force model (Th 2.140, U 2.055, Np 2.042, Pu 2.029, Am 2.017 Å) [29], i.e., the bond lengths deviate on average by 0.039 Å (1.9%). So the 5f-in-core approximation holds quite well for the tetravalent PPs, although the calculated SPP 5f occupations are about 0.22 electrons larger than the integral LPP occupations. The reason why this approximation still works is the f-part of the LPPs, which sufficiently account for the 5f participation in chemical bonding, i.e., the LPP 5f occupations attain values up to 0.27 electrons, and thus the differences between the LPP and SPP 5f occupation only amount to ca. 0.07 electrons.

The use of LPPs in combination with CPPs yields about 0.007 Å smaller bond lengths related to pure LPP HF calculations. Therefore the deviations from SPP calculations are reduced by about 30% compared to those using pure LPPs, i.e., the m.a.e. (m.r.e.) decreases from 0.018 (0.9%) to 0.012 Å (0.6%). The comparison to the experimental respectively estimated data shows only a slight improvement, if CPPs are used, i.e., the m.a.e. (m.r.e.) decrease from 0.034 (1.7%) to 0.030 Å (1.5%).

The introduction of correlation via CCSD(T) shortens the An–F distances by 0.006 and 0.003 Å for ThF_4 and UF_4 , respectively. The differences between LPP CCSD(T) calculations and experimental data amount to $-0.023/+0.032$ Å for ThF_4/UF_4 , and are thus slightly larger respectively smaller than those between LPP HF calculations and the experiment ($-0.017/+0.035$ Å for ThF_4/UF_4). The use of CPPs on the CCSD(T) level has only a small effect on the An–F bond length, i.e., the Th–F and U–F bond length is shortened by 0.004 and 0.003 Å, respectively. Therefore the deviation to the experiment also changes only slightly, whereby it becomes larger respectively smaller for ThF_4 and UF_4 ($-0.023/-0.027$ and $+0.032/+0.029$ Å for LPP/LPP+CPP of ThF_4 and UF_4).

3.2.2 Actinide–fluorine bond energy

The An–F bond energies decrease by 0.51 and 0.53 eV from ThF_4 to CfF_4 for LPP and SPP calculations, respectively. This is due to the increasing fluorine–fluorine repulsion with decreasing An–F distances as it is the case for AnF_2 . While

the LPP HF bond energies decrease smoothly, the SPP data show a minimum for BkF_4 , i.e., for a half-filled 5f shell.

The LPP HF bond energies deviate at most by 0.151 eV (3.0%) from SPP reference data except for BkF_4 , for which the difference is 0.238 eV (4.9%). However, this high deviation is reduced to 0.049 eV (0.7%), if LPP and SPP CCSD(T) single point calculations at the optimized HF BkF_4 structures are compared (CCSD(T) results: 6.604/6.653 eV for LPP/SPP; frozen orbitals: F 1s for LPP and F 1s, An 5s 5p 5d for SPP). Taking the BSSE into account this deviation is even further decreased to 0.037 eV (counterpoise corrected CCSD(T) results: 6.507/6.470 eV for LPP/SPP). To investigate the correlation effects single point CCSD(T) calculations were considered to be sufficient, since the AnF_4 structures are only slightly affected by using CCSD(T) instead of HF (bond length decrease by at most 0.006 Å). For the other elements (Th–Cm, Cf) at the HF level the m.a.e. (m.r.e.) amounts to 0.064 eV (1.2%) and the largest deviations occur for Am (0.095 eV) and Cm (0.151 eV), where the differences between the LPP and SPP 5f occupation achieve their maximum (0.10/0.09 electrons for Am/Cm).

The application of CPPs affects the bond energies only very slightly and the deviations compared to the SPP data remain almost equal, i.e., without BkF_4 the m.a.e. (m.r.e.) is 0.063 (1.2%). The change from LPP HF to LPP CCSD(T) calculations results in a strong increase of the bond energies by 1.500 and 1.502 eV for ThF_4 and UF_4 , respectively. The use of LPPs in connection with CPPs at the CCSD(T) level causes for both ThF_4 and UF_4 only a small increase in bond energy by 0.035/0.026 eV.

3.3 Range of applications

The 5f-in-core PPs proposed here (di- and tetravalent actinides) as well as those of a previous publication (trivalent actinides) [8] simplify electronic structure calculations on actinide compounds significantly. However, the assumption of a fixed near-integral 5f occupancy also bears the danger of misuse of the approach, e.g., for cases where another 5f occupancy than modeled by the PP is actually present, cases where states with different 5f occupancies mix, or systems where the 5f orbitals strongly contribute directly to chemical bonding in a MO-LCAO (molecular orbitals by linear combination of atomic orbitals) sense. Thus, we urge the users of the 5f-in-core PPs to verify the underlying assumption by (single point) test calculations using, e.g., 5f-in-valence SPPs [6,7] or AE methods at the HF level. It is clear that questions related to individual electronic states cannot be addressed with the present approach, which rather provides answers for an average over a multitude of states characterized by the same 5f occupancy and the same valence substate, i.e., a superconfiguration in the sense of the concept of Field advocated for lanthanides more than two decades ago [30].

Besides the systems studied here we see applications of the 5f-in-core PPs for divalent actinides, for example, in the study of metal clusters of heavier actinides, similar to previous related work on ytterbium clusters [31]. In case of tetravalent actinides the bis-cyclooctatetraene complexes have been successfully investigated with 5f-in-core PPs, which were found to be able to model quite well the contributions of f and d orbitals to metal–ring bonding (yet unpublished results). In addition a couple of applications have been published for 5f-in-core PPs modeling trivalent actinides [9,10]. In summary we think that the range of possible successful applications of the actinide 5f-in-core PPs is certainly somewhat smaller than for lanthanide 4f-in-core PPs [11], nevertheless, a quite significant part of actinide chemistry remains open for applications of the approach.

4 Conclusion

Quasirelativistic 5f-in-core PPs and corresponding optimized valence basis sets have been presented for di- and tetravalent actinide atoms and proved to be reliable tools for molecular calculations as long as the 5f occupancy is near-integral. Atomic HF calculations using our newly developed PPs and basis sets deviate by less than 0.2 eV from corresponding numerical quasirelativistic AE HF results. The differences using any respectively the VQZ contraction of the (7s6p5d) basis set stay below 0.1 eV for divalent and tetravalent PPs.

Results of HF test calculations on AnF_2 (An = Pu–No) and AnF_4 (An = Th–Cf) using 5f-in-core LPPs show reasonable agreement with corresponding 5f-in-valence SPP calculations except for PuF_2 – CmF_2 and the bond energy of BkF_4 , i.e., the m.a.e. (m.r.e.) in bond lengths and energies amount to maximal 0.02 Å (0.9%) and 0.09 eV (2.5%). The higher deviations for PuF_2 – CmF_2 are due to a strong configurational mixing of $5f^{n+1}$ and $5f^n 6d^1$, whereby the assumption of a near-integral 5f occupation is too crude. The reason for the large difference in the bond energy of BkF_4 are correlation effects within the 5f shell, which cause a too small SPP bond energy.

The adjusted CPPs improve the LPP HF results, i.e., the decrease in deviations related to SPP data amounts to 0.012/0.006 Å and 4.1° for the bond lengths of AnF_2 / AnF_4 and the bond angles of AnF_2 , respectively. The HF An–F bond energies are not affected (AnF_4) or even get worse (AnF_2) due to the inclusion of dynamic correlation by using CPPs. However, at the correlated level the CPP method is reasonable, e.g., the difference to the SPP CCSD(T) bond energy of NoF_2 is reduced from 0.026 to 0.017 eV by using the CPP correction.

Finally, we want to emphasize again that the derived 5f-in-core PPs will only lead to reasonable results for those cases

where the An 5f occupation number is close to integral. We recommend to explicitly test this condition, e.g., in single-point HF calculations with an explicit treatment of the 5f shell.

References

1. Katz JJ, Seaborg GT, Morss LR (1986) The chemistry of the actinide elements, Vol 2. Chapman and Hall, London
2. Pepper M, Bursten B (1991) Chem Rev 91:719
3. Schreckenbach G, Hay PJ, Martin RL (1999) J Comp Chem 20:70
4. Dolg M, Cao X (2003) The relativistic energy-consistent ab initio pseudopotential approach. In: Hirao K, Ishikawa Y (eds) Recent advances in relativistic molecular theory. World Scientific, New Jersey
5. Cao X, Dolg M (2006) Coord Chem Rev 250:900
6. Küchle W, Dolg M, Stoll H, Preuss H (1994) J Chem Phys 100:7535
7. Cao X, Dolg M, Stoll H (2003) J Chem Phys 118:487
8. Moritz A, Cao X, Dolg M (2007) Theor Chem Acc 117:473
9. Cao X, Li Q, Moritz A, Xie Z, Dolg M, Chen X, Fang W (2006) Inorg Chem 45:3444
10. Wiebke J, Moritz A, Cao X, Dolg M (2007) Phys Chem Chem Phys 9:459
11. Dolg M, Stoll H, Savin A, Preuss H (1989) Theor Chim Acta 75:173
12. Dolg M, Stoll H, Preuss H (1989) J Chem Phys 90:1730
13. Froese Fischer C (1977) The Hartree–Fock method for atoms. Wiley, New York; program MCHF77, modified for pseudopotentials and quasirelativistic calculations by Dolg M (1995)
14. Dolg M, Stoll H, Preuss H (1993) Theor Chim Acta 85:441
15. Wang Y, Dolg M (1998) Theor Chem Acc 100:124
16. Müller W, Flesch J, Meyer W (1984) J Chem Phys 80:3297
17. Müller W, Meyer W (1984) J Chem Phys 80:3311
18. Kolb D, Johnson WR, Shorer P (1982) Program package to calculate electric and magnetic susceptibilities and shielding factors for closed-shell atoms and ions of high nuclear charge. University of Kassel
19. Amos RD, Bernhardsson A, Berning A, Celani P, Cooper DL, Deegan MJO, Dobbyn AJ, Eckert F, Hampel C, Hetzer G, Knowles PJ, Korona T, Lindh R, Lloyd AW, McNicholas SJ, Manby FR, Meyer W, Mura ME, Nicklass A, Palmieri P, Pitzer R, Rauhut G, Schütz M, Schuhmann U, Stoll H, Tarroni AJSR, Thorsteinsson T, Werner HJ (2002) MOLPRO is a package of ab initio programs. University of Birmingham
20. Pitzer RM (1979) Atomic electronic structure code ATMSCF. The Ohio State University, Columbus
21. Dunning TH Jr (1989) J Chem Phys 90:1007
22. Kendall RA, Dunning TH Jr, Harrison RJ (1992) J Chem Phys 96:6769
23. Girichev GV, Krasnov KV, Giricheva NI, Krasnova OG (1999) J Struct Chem 40:207
24. Konings RJM, Hildenbrand DL (1998) J Alloys Compd 271:583
25. Dolg M, Stoll H (1989) Theor Chim Acta 75:369
26. Dyllal KG, Grant IP, Johnson CT, Parpia FA, Plummer EP (1989) GRASP: atomic structure code. Comput Phys Commun 55:425
27. Wang SG, Schwarz WHE (1995) J Phys Chem 99:11687
28. Mochizuki Y, Tatewaki H (2003) J Chem Phys 118:9201
29. Akdeniz Z, Karaman A, Tosi MP (2001) Z Naturforsch 56:376
30. Field RW (1982) Ber Bunsenges Phys Chem 86:771
31. Wang Y, Schautz F, Flad HJ, Dolg M (1999) J Phys Chem A 103:5091